JOURNAL OF ORTHOPAEDICS 12 (2015) S51–S61

Available online at www.sciencedirect.com

ScienceDirect

journal homepage: www.elsevier.com/locate/jor

Original Article

The healing stages of an intramedullary implanted tibia: A stress strain comparative analysis of the calcification process

*Vincenzo Filardi**

CARECI, University of Messina, 98100 Messina, Italy

ARTICLE INFO

Article history:
Received 18 June 2014
Accepted 4 January 2015
Available online 31 January 2015

Keywords:
Stress on tibia
Close tibial shaft fracture
Unreamed intramedullary tibial nails

ABSTRACT

Aims: The extended usage of unreamed tibial nailing resulted in reports of an increased rate of complications, especially for the distal portion of the tibia. Unreamed nailing favours biology at the expense of the achievable mechanical stability, it is therefore of interest to define the limits of the clinical indications for this method. Extra-articular fractures of the distal tibial metaphysis, meta-diaphyseal junction, and adjacent diaphysis are distinct in their management from impaction derived "pilon" type fractures and mid-diaphyseal fractures. The goals of this work were to gain a thorough understanding of the load-sharing mechanism between unreamed nail and bones in a fractured tibia. With this purpose a complete model of the human leg was realised, simulating a mid-diaphyseal fracture, classified as A2 type 1, according to the AO classification.

The analysis of the entire chain allows to have a complete picture of the stress distribution and of the most stressed bones and soft tissues, but, more importantly can overcome problems connected with boundary conditions imposed at single bony components.
Methods: Model consists of six bony structures: pelvis, femur, patella, fibula, tibia, and a simplified lump of the feet, configured in a standing up position. Their articular cartilage layers, were simulated by 3D membranes of opportune stiffness connecting the different segments. Moreover an unreamed intra-medullary nail Expert Tibial Nail (DePuy Synthes®) stabilized the fractured tibia. A load of 700 N has been applied at the top of pelvis and a part the feet, at the tip, was rigidly fixed. Five different contact interfaces have been imposed at the different bony surfaces in contact.
Results: Three different conditions were analysed: the initially healthy tibia, the A2 type 1 fractured tibia with the Expert tibial nail implanted, and the follow up stage after complete healing of tibia. Non-linear finite element analysis of the models were performed with Abaqus version 5.4 (Hibbitt, Karlsson and Sorensen, Inc., Pawtucket, RI) using the geometric non linearity and automatic time stepping options.
Conclusion: The obtained results reveal interesting consequences deriving by taking into account how the stress shielding can influence the integrity and resistance of bones, in order to identify the mechanical reasons for the unfavourable clinical results, and to

* Tel.: +39 0906768264.
E-mail address: vfilardi@unime.it.
http://dx.doi.org/10.1016/j.jor.2015.01.016

identify borderline indications due to biomechanical factors. The evolution of treatment options for these fractures has been closely linked to developments in implant technology and surgical technique. Further developments in this area, particularly with respect to minimally invasive plating techniques and nail design are ongoing.

1. Introduction

The tibia is the most commonly fractured long bone in the body; the hospital implies a long recovery period and high ratio of permanent morbidity,[1] for this reason, it is important to determine the best treatment for these injuries. The potential management may include both operative and non-operative options; the choice of treatment will depend upon patient factors, the extent of soft-tissue injury, the fracture configuration, available equipment and surgical experience. Intramedullary nailing has been established as a reliable method for the treatment of fractures of the tibial shaft. This technique has been reported as highly successful in terms of fast union, good alignment, low shortening, good functional results, and low complication rates.[2] For decades, nails have been the most frequently used stabilizers for the surgical treatment of dia/metaphyseal fractures. They have been greatly improved in recent years and their indications have been widely extended.[3] The choice of the osteo-synthesis device has thereby become an issue of special interest since the local mechanical behaviours originated in the bone by the fixation system may influence the process of bone healing.[4] The mechanical environment generated by the osteo-synthesis provides an essential stimulus for new bone formation.[5] It has been shown that a certain amount of inter-fragmentary movement stimulates callus formation,[4,6] and healing rate.[7] The advent of the interlocked tibial nail increased the indication for intramedullary fixation to include most non articular tibial fractures. The range of indications has been extended as far as the metaphyseal border of the proximal shaft.[8] The stiffness of the fixation system has a substantial influence on the progress of healing, and the mechanism of load sharing between bone and fixation device may influence the longevity of the osteo-synthesis. An alteration of bone loading after osteo-synthetic stabilization is expected on the local as well as on the global level. Considerable controversy exists concerning the advantages of reaming or non-reaming in the treatment of tibial diaphyseal fractures with intramedullary nails. Indeed, the unreamed nail was developed to address the lack of blood supply near the fracture.[9,10] Tibial fractures, especially distal ones, have poor soft tissue coverage and external blood supply.[11] Reaming destroys the medullary blood supply, while unreamed tibial nailing has a lower impact on the endosteal blood supply.[9] The disadvantage of unreamed tibial nails is their less tight fit when compared to reamed ones, which results in a higher incidence of malunion.[12] Court- Brown et al[13] performed a study of the tibial diaphyseal fractures, comparing the reamed Grosse-Kempf tibial nail with the unreamed AO UTN nail. There was no malunion in the reamed group, while four cases occurred in the unreamed group, in which 13 patients had screw breakage and one had a broken nail. Due to fracture stabilization, extended portions of the bone may become subjected to unloading or overloading. In the long term, this may lead to bone resorption and remodelling.[14] Within the fixation system, high stresses and fatigue can lead to its technical failure. Compression, bending, and torsional tests have been performed to compare the stiffness and fatigue behaviour of various interlocking nails,[15] or implanted nails.[16] These studies provide precious information on the overall stability of the implant–bone complex. However, they do not permit an assessment of the appropriateness of a fixation device in vivo. Stiffness tests seldom provide information on the alteration of bone loading due to fracture fixation.[17] But as long as these tests use simple compression or torsional loads, the load sharing between implant and bone under physiological conditions remains unknown. Clinical reports,[18] indicate an increased incidence of mechanical failures in the unreamed nailing of distal tibial fractures (17.9%) compared with the other regions of the lower leg (14%). The extension of indications for unreamed tibial nailing to the metaphyseal regions of the bone resulted in reports of increased complication rates.[19,20] While indications in the proximal third are known to be associated with surgical problems,[21] there are no surgical restrictions on use in the distal third. Different computational models have been used to study tibial fractures. Raunest et al[22] performed a 3D finite element (FE) model of the human tibia to analyse the biomechanical effects caused by an unreamed interlocking nail (UTN) for different types of tibial fractures. In that work, the anchorage of the implant in trabecular bone was simulated with elastic rods. Duda et al[23] also developed a FE tibial model to study the performance of the UTN. They performed a more accurate 3D FE model simulating both cortical and trabecular bone and considered the interface between implant and bone with corresponding contact elements with null friction. They analysed up to five different fracture locations and concluded that the clinical problems reported for distal fractures might be due to less favourable mechanical conditions. Fibular osteosynthesis has been used as a method to enhance the treatment of tibial fractures.

However, none of the above computational models considered the influence of the fibula and the interosseous membrane (IOM), though some authors think they play a mechanical role in stabilizing tibial fractures.[24] Many works have been performed to clarify the role of the fibula and IOM in

load transfer in the lower extremity,[24–26] though differing conclusions have been drawn. Lambert[26] reported that 15% of load transmitted by the lower leg is carried by the fibula. Sonoda et al[27] performed a 3D FE model of the tibio–fibula complex, including the IOM, by means of gap elements in a study of stress fractures in athletes. We know of no FE simulation that models the complete interaction among tibia, fibula, and IOM system including intramedullary nails. In this work, two different nails, an unreamed medullary interlocking nail and a reamed medullary interlocking nail, have been studied from a biomechanical point of view to determine their ability to stabilize different shaft fractures of the tibia (proximal, mid-diaphyseal, and distal). The risk of fracture of these nails and their bolts and the role of the fibula and IOM on the stabilization of these fractures were also studied. Beside variations in mechanical conditions, a number of additional factors might have contributed significantly to the reported clinical outcome. First of all, the injury mechanisms are quite different in proximal (impact) versus distal fractures (torsion) of the tibia. This may result in differences in the clinical outcome.[28,29] Additional injuries may considerably alter the long-term outcome for tibial fractures.[30] While the mechanism of injury cannot be influenced by the clinician, the osteosynthesis may be optimized to support the biological healing process. Thus a better understanding of the load and strains sharing, between implant and bone, may encourage the healing process. The goals of this work is to investigate by using a complete 3d FE model of the leg the load sharing mechanism between implant and bone in a fractured tibia under physiological loading, to identify mechanical reasons which could act to generate the failure of the nail.

2. Materials and methods

The geometrical data of the model developed herein were obtained by matching a nuclear magnetic resonance (MRI) for soft tissues, and a computerized tomography (CT) for bones, with images taken from a normal adult patient, separated at intervals of 1.5 mm in the sagittal, coronal and axial planes with the knee at 0° flexion (accuracy 0.5 mm). These lines were transferred into the commercial code Hypermesh by Altair® where the main surfaces and solid version of the model were reconstructed; in particular 5.758 elements and 1.837 nodes were used for pelvis, 20.096 elements and 1.012 nodes in femur, 2.567 elements and 687 nodes in patella, 2.480 elements and 849 nodes in fibula, 17.831 elements and 2.032 nodes in tibia and 1.120 elements and 412 nodes for the foot. On the upper

Fig. 1 – The Orthopaedics Trauma Association (OTA) A0 classification of tibial diaphyseal fractures, the chosen case was A2 type 1.

zone, the ilio-femoral ligament, the ligament of the hip joint, which extends from the ileum to the femur in front of the joint, was modelled with 252 tetrahedral elements and 151 nodes. The knee joint constituted by the medial collateral ligament, which extends from the medial femoral epicondyle to the tibia, the lateral collateral ligament, which extends from the lateral femoral epicondyle to the head of the fibula, the anterior cruciate ligament which extends postero-laterally from the tibia and inserts on the lateral femoral condyle, and the posterior cruciate ligament which extends antero_medially from the tibia posterior to the medial femoral condyles were modelled with 529 tetrahedral elements and 296 nodes. On the lower zone, the foot joint, constituted by the plantar fascia, the medial and lateral ligaments were modelled with 366 tetrahedral elements and 187 nodes. For tibia, and other bony parts of the model, material properties were distinguished between two principal regions, cortical bone and trabecular bone. The mechanical properties were assumed to be linear elastic, isotropic and homogeneous. Young's modulus of trabecular bone grew from 300 to 700 MPa over three element layers from proximal to distal.[31] Young's modulus of the compact bone was selected to be E = 17.000 MPa with a Poisson's ratio of n = 0.3[32,33]; A mid-diaphyseal fracture classified as A2 type 1, see Fig. 1, was simulated on tibia, according to the AO classification.[34] No contact and a gap size of 9 mm, between fracture fragments, were imposed. An unreamed intra-medullary nail Expert Tibial Nail (*DePuy Synthes*®) stabilized the fractured tibia. The shape of the medullary cavity defined the nail position within the cavity of the model tibia (Fig. 2). The Expert Tibial Nail (http://footandanklefixation.com/product/synthes-expert-tibial-nail/) permits an intra-medullary approach for the fixation of proximal, shaft and distal fractures of the tibia, providing a stable fixation of fractures by incorporating oblique locking holes in the proximal and distal portions of the nail. An intra-medullary approach results in decreased blood loss compared to plate fixation. Cancellous bone locking screws are used proximally for better purchase in the cancellous bone. The most proximal locking screw, when used with an end cap, provides a locked, fixed-angle construct, prevents in growth of tissue and facilitates nail extraction. Three unique and innovative locking options, in combination with cancellous bone locking screws, increase the stability of the proximal fragment for proximal third fractures. Two state of the art medio-lateral (ML) locking options enable primary compression or secondary controlled dynamization of proximal fractures. Locking screws in the distal oblique hole and ML hole provide stable fixation of distal fractures. Diameters ranging from 8 mm to 13 mm (1 mm increments), in particular a diameter of 10 mm has been chosen in our case. From 8 mm to 10 mm nails have a proximal diameter of 11 mm and are round, while they have a proximal diameter consistent with the shaft diameter and are fluted, for the other sizes. Length can vary from 255 mm to 465 mm (15 mm increments); in our case it is 330 mm. Three distal (L = 38 mm, ϕ = 4 mm) and two proximal (L = 35 mm, ϕ = 4 mm) interlocking bolts were used to stabilize the bony fragments of the investigated tibial fracture, see Fig. 2. Titanium alloy was selected as the material for nails and bolts (Ti–6Al–7Nb), modelled as linear elastic, isotropic and homogeneous with the Young's modulus and Poisson's ratio of E = 110.000 MPa and ν = 0.3 respectively. Contact interfaces were imposed at the ilio-femoral (femur-pelvis), knee (femur-patella, patella-tibia, and fibula-tibia) and foot (tibia-feet) joints; defined using a penalty-based method with a weight factor, a coefficient of friction of 0.04 was chosen to be consistent. The glue option

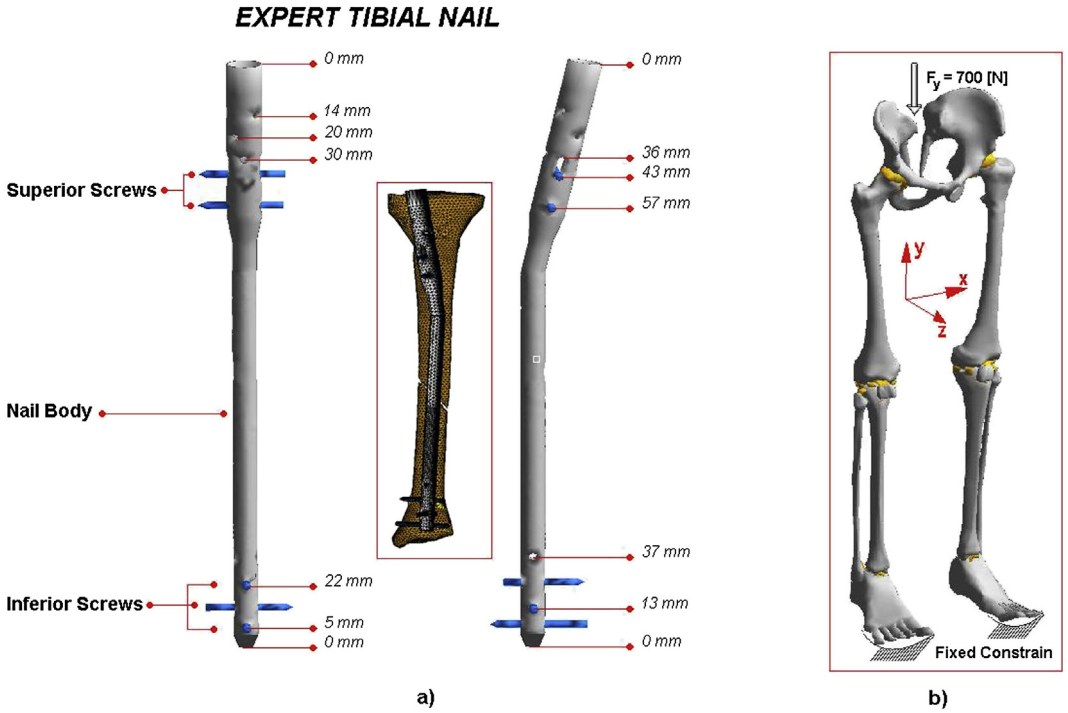

Fig. 2 – a) Geometrical characteristics of the implant and FE model representation. b) loading and constrain conditions appled to the FEB simulation.

was chosen to simulate the contact interface between nail, screws, and tibial bony fragments. A distributed, on 70 nodes, vertical (y axes) load of 700 N was applied on the left side of the pelvis, while a fixed constrain, of 200 nodes, was imposed at the lower extremity of the foot, see Fig. 2.

A mid-diaphyseal fracture, classified as A2 type 1, according to the AO classification, was simulated on the left tibia and Different conditions were analysed: the A2 type 1 fractured and separated tibia with the Expert tibial nail implanted (initial condition), and the follow up stages until the complete healing of tibia, by percentage increasing of the Young Modulus. Finally the results have been compared with those of a healthy tibia.

Non-linear finite element analysis of the models were performed with Abaqus version 5.4 (Hibbitt, Karlsson and Sorensen, Inc., Pawtucket, RI) using the geometric nonlinearity and automatic time stepping options.

3. Results

A geometrical accurate 3D FE model of the human complete model of the leg was realised. The analysis of the entire chain allows having a complete picture of the stress and strain distribution, but, more importantly can overcome problems connected with boundary conditions imposed at single bony components. By analysing the obtained results a simple consideration must be done, for a value corresponding at 10% (1700 MPa) of the elastic modulus, stresses, displacements, and strains, solicited the implanted calcifying bone in almost the same condition of an implanted and completely healed tibia. For this reason, by supposing a healing period of 180 days, each percentage of the increased Young Modulus was associated to a specific interval of days. In Table 1 are reported the obtained results in terms of the maximum equivalent Von Mises Stress, displacements, and equivalent elastic strain, localised on the nail body, on the two superior screws, and on the inferior distal screws. The eq. Von Mises Stresses, see Fig. 3, follow a regular decreasing trend with values ageing from about 160 to 95 MPa on the nail body, the two superior screws suffer a stress from about 36 to 31 MPa for the case of the fractured tibia, to arrange their stress distribution on the value of about 31 MPa for the remaining cases. The three inferior screws result unloaded for the case of the fractured tibia (13.54 MPa), to follow an increasing of the stress until 34 MPa. Displacements on the nail body reach their maximum value of 6.2 mm at the 1% (170 MPa) of the value imposed to the elastic modulus of the tibia, to follow a decreasing trend till 5.37 mm until the complete calcification of the fracture, (E = 17000 MPa). The same considerations, reported for the nail body, can be done for the superior screws which show a maximum displacement of 4.61 mm for the 1% of the Elastic modulus. The final value, at the consolidation of the fracture, is of 4.05 mm. Displacements on the inferior screws follow a decreasing trend, from the fracture to the complete consolidation, with values ageing from 0,38 to 0.35 mm. The equivalent elastic strain on the nail body has a peak in the case of the fractured tibia 67 [mΣ], and then follows an increasing trend from 50 to 52 [mΣ]. The equivalent elastic strain registered on the superior and inferior screws follow increasing

Table 1 – Results in terms of Eq. V. Mises Stress, Displacements, and Eq. Elastic Strain localised on the body nail and screws.

Days	E%	E [MPa]	Eq. V. Mises on Nail [MPa]	Eq. V. Mises on sup. Screws [MPa]	Eq. V. Mises on inf. Screws [MPa]	Displ. on nail [mm]	Displ. on sup. screws [mm]	Displ. on inf. screws [mm]	Eq. El. strain on nail [mΣ]	Eq. El. strain on sup. screws [mΣ]	Eq. El. strain on inf. screws [mΣ]
0	0%	0	159.9	36.44	13.54	5.14	3.67	0.38	67	11	8
25	1%	170	119.4	30.74	31.24	6.21	4.61	0.36	50	21	23
45	10%	1700	96.71	31.05	33.6	5.51	4.14	0.35	51	25	25
60	20%	3400	95.89	31.14	33.78	5.45	4.1	0.35	51	25	25
75	30%	5100	95.58	31.16	33.85	5.42	4.08	0.35	51	26	25
90	40%	6800	95.4	31.17	33.9	5.41	4.07	0.35	52	26	25
105	50%	8500	95.28	31.17	33.93	5.4	4.06	0.35	52	26	25
120	60%	10200	95.19	31.18	33.95	5.39	4.06	0.35	52	26	25
135	70%	11900	95.12	31.19	33.97	5.38	4.05	0.35	52	26	25
150	80%	13600	95.07	31.19	33.98	5.38	4.05	0.35	52	26	25
165	90%	15300	95.02	31.19	34	5.37	4.05	0.35	52	26	25
180	100%	17000	94.99	31.2	34	5.37	4.05	0.35	52	26	25

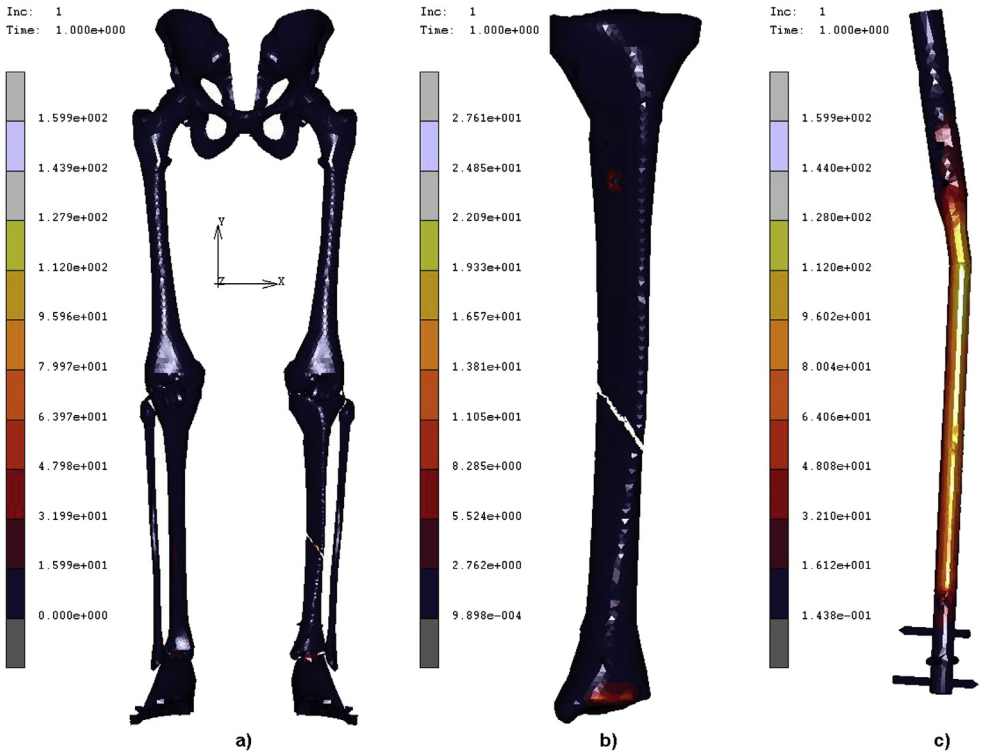

Fig. 3 – Contour maps of the Eq. V.Mises stress localized on a) the complete model b) the fractured tibia c) Expert tibial nail.

courses respectively ageing from 11 to 26 [mΣ], for the superior screws, and from 8 to 25 [mΣ] for the inferior ones. In Table 2 are reported the obtained results in terms of the maximum equivalent Von Mises Stress, displacements, and equivalent elastic strain, localised on the complete model, on the fractured tibia, and on the calcifying fractured area. The eq. Von Mises Stresses follow a regular decreasing trend, see Fig. 3, with values ageing from about 160 to 95 MPa on the complete model, as seen for the nail body. On the fractured tibia, apart the initial condition with 27 MPa, the eq. Von Mises Stresses follow a regular decreasing trend from 43 to 40 MPa, see Fig. 4. The last value is almost totally reached at 45 days of course. On the zone of the calcifying fractured area, no stress can be found at the initial condition, while a decreasing trend can be individuated until 60% (120 days) of the elastic modulus (values ageing from 16 to 11 MPa). At 70% of the Elastic Modulus (135 days) trend starts to increase reaching a value of about 12 MPa, at 100% of Elastic Modulus. No significant differences can be evidenced for the Global displacements localised on the fracture (1.72 mm), see Fig. 5–6, and Table 2. In order to better understand the mechanism of calcifying of the fracture both positive and negative displacements along the Y axes, see Fig. 6; were calculated around the described area. The results indicate a decrement, reached at 20% of Elastic modulus (60 days), of both positive and the negative displacements, ageing from +0.20 to +0.15 mm and −0.37 to −0.29 mm respectively. The equivalent elastic strain, see Fig. 7, as expected registers a decreasing trend on the tibia ageing from 154 to 222 [mΣ], and from 0 to 63 [mΣ] on the fracture site. Finally a comparison between the healthy tibia and the fractured one, in terms of eq. V. Mises Stress is proposed in Fig. 8.

4. Discussion

The fixation of distal tibial fractures with intra-medullary nails is associated with high union rates and offers a significant benefit in not disturbing the soft-tissue envelope at the fracture site. However the use of this technique in distal tibial fractures has historically been associated with reports of malunion often due to technical problems including difficult fracture reduction, fracture propagation into the ankle joint, hardware failure, and inadequate distal locking options.[35–37] A number of implant and surgical advances have been developed over the past two decades to improve implant durability and aid fracture reduction. Achieving and maintaining a good reduction is the most difficult aspect of nailing distal tibial meta-diaphyseal fractures. In mid-diaphyseal fractures, insertion of the intramedullary nail aids fracture reduction as the nail has a diameter only slightly smaller than the cavity in which it sits, ensuring coronal and sagittal alignment. The hypothesis of the present work was that a better understanding of the load sharing between implant and bone may help to understand the mechanical aspects of the healing process in a tibia stabilized with an unreamed nail. The analysis of the intact tibia, under physiological like and simplified loading conditions, allowed investigation of the surface strain distribution. Simplified loading significantly overemphasized bending in the distal portion of the tibia. This further stresses the assumption that, beside their capability to allow relative movements in joints, muscles play a major role in compensating shear and bending loads which would otherwise lead to an overloading of the long bones.[38–40] The analysis of the fractured tibia revealed a considerable

Table 2 – Results in terms of Eq. V. Mises Stress, Displacements, and Eq. Elastic Strain localised on the complete model, on the fractured tibia, and on the fracture.

Days	E%	E [MPa]	Max Eq. V. Mises on Model [MPa]	Max Eq. V. Mises on tibia [MPa]	Max Eq. V. Mises on fract. [MPa]	(+) Y Displ. on fract. [mm]	(−) Y Displ. on fract. [mm]	Tot. displ. on fract. [mm]	Eq. El. strain on tibia [mΣ]	Eq. El. strain on fract. [mΣ]
0	0%	0	159.90	27.61	0.00	0.00	0.00	0.00	154	0.00
25	1%	170	119.40	43.25	15.70	0.20	−0.37	1.71	1810	1810
45	10%	1700	96.71	40.80	12.82	0.16	−0.30	1.71	307	307
60	20%	3400	95.89	40.57	12.15	0.15	−0.29	1.72	221	191
75	30%	5100	95.58	40.48	11.88	0.15	−0.29	1.72	222	145
90	40%	6800	95.40	40.43	11.65	0.15	−0.29	1.72	222	119
105	50%	8500	95.28	40.39	11.47	0.15	−0.29	1.72	222	102
120	60%	10200	95.19	40.37	11.31	0.15	−0.29	1.72	222	89
135	70%	11900	95.12	40.35	11.35	0.15	−0.29	1.72	222	80
150	80%	13600	95.07	40.33	11.48	0.15	−0.29	1.72	222	73
165	90%	15300	95.02	40.32	11.63	0.15	−0.29	1.72	222	67
180	100%	17000	94.99	40.31	11.82	0.15	−0.29	1.72	222	63

unloading of the tibia compared with the intact condition, see Fig. 8. The unloading was very pronounced for the distal defect. In the antero-lateral cortices, the tension was slightly enhanced. The load sharing between implant and bone led to an axial loading of the nail and an unloading of the bone between the proximal and distal interlocking bolts, see Table 1. The bone itself was mainly loaded under bending. On the side of the defect, the bending moments were transferred through bone–nail contact interfaces. This contact between bone and nail resulted in an unloading of the bone (Fig. 8 and Table 2) and an increase in the loading of the nail at the fracture site (Fig. 3). Loads were transferred through the locking bolts, the contact through the trabecular bone, and through contact forces at the level of the defect. Due to the extremely low Young's modulus at the defect site, only negligible forces were directly exchanged between the bone and nail at the defect site. On one side, the nail was statically locked between the proximal and distal interlocking bolts. Major load transfer took place through the bolts and resulted in an unloading of the interlocked bone segment (Figs. 3 and 8). On the other side, the unloading was somewhat compensated by contact pressures which are transferred from the implant through the inner cortex to the bone.

The stress distribution in the nail was characterized by bending superimposed onto axial compression and torsion. In the region across the defect, the nail showed an intensive loading along the anterior and posterior edges, mainly due to bending. The postero-medial and antero-lateral aspects of the nail were less loaded than the anterior and posterior edges. The high axial stiffness of the nail restrained inter-fragmentary motion. The inter-fragmentary shear movement was mainly due to the relative rotation of the bony fragments around the longitudinal axis of the tibia. A finite element analysis by Gomez-Benito et al[41] compared the biomechanical performance of reamed and unreamed tibial nails. They concluded that reamed nails were superior to unreamed nails in mid-diaphyseal and distal tibial fractures as lower stresses were transmitted to the locking screws, reducing the risk of screw failure. In distal tibial fractures, treated by the GrossKempf nail, the role of distal locking is not just to control length and rotation, but also stability in the coronal and sagittal planes.

A clear stress concentration was always visible in the neighbourhood of the insertion of the screws. The maximum nail stresses were observed with a proximal fracture in the unreamed nail and with a distal fracture and a reamed nail, with values of 230 and 275 MPa, respectively. The computed von Mises stresses in the bolts of unreamed nails for the distal and mid-diaphyseal fractures were about 590 MPa. In general, it is expected that the stress level would decrease during the fracture healing process due to the increasing stiffness of the fracture callus. Gomez-Benito et al[41] considered the gap completely healed, and obtained a von Mises stress in the bolts of the unreamed nail of 160 MPa. In this paper a different nail, and different loading conditions, were adopted, thus the obtained results report eq. Von Mises Stresses values ageing from about 160 to 95 MPa on the nail body, and a stress of about 36 MPa on the two superior screws for the case of the fractured tibia, which stabilizes to the value of about 31 MPa for the remaining cases, until the complete healing. The three inferior screws result unloaded for the case of the fractured

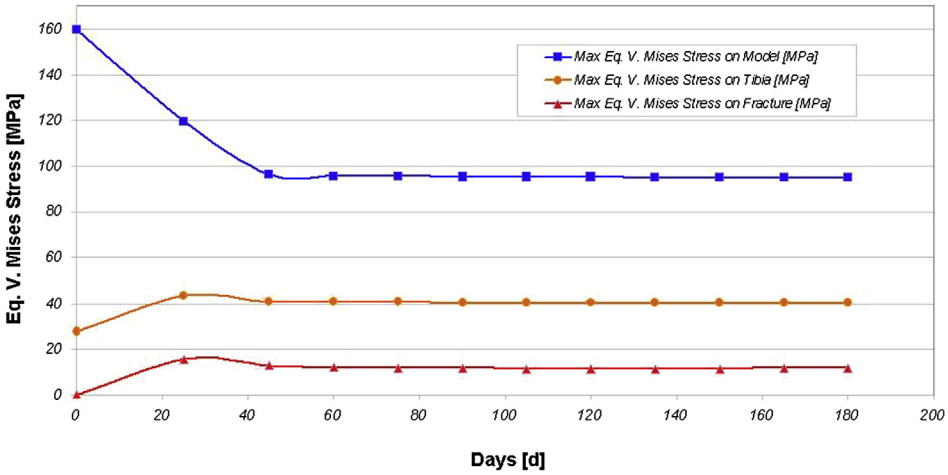

Fig. 4 – Curves of Eq. Von Mises stress Vs Days (or equivalent percentage of the elastic modulus) for the complete model fractured tibia, and fracture.

tibia until 13,54 MPa, then follow an increasing of the stress until 34 MPa. The obtained results must be interpreted by considering we have used a complete FE model taking into account the complete bony chain of the leg, much less rigid of a single constrained and implanted tibia. Unreamed nailing of the distal defect results in an extremely low axial and high shear strain between the fragments. The simultaneous presence of low axial and high shear strains is viewed critically from a clinical point of view.[42–44] Apart from biological reasons, clinical problems reported for distal fractures may be due to the less favourable mechanical conditions in unreamed nailing. In a clinical setting, the aim is to reduce large defects. This would lead to an unloading of the nail and to compression of the fracture fragments. In all proximal and diaphyseal defect locations, considerable axial and shear interfragmentary strains were evident. Measurements on fracture gap movements in humans show strain values as large as 50% and more in external fixation.[45] Compared with external fixation, a rigid medullary stability achieved through nailing avoids excessively large interfragmentary strains. Fractures are usually reduced or dynamized and bone contact exists between fracture fragments. This reduces the axial movement component dramatically. In contrast, reduction or dynamization does not necessarily reduce shear movements. Only with sufficient bone contact, (i.e., friction between fragments and axial loading), the shear movement is reduced or avoided. A possible explanation for the negative effect of a large axial to shear ratio might be that fractures are hardly stabilized if they

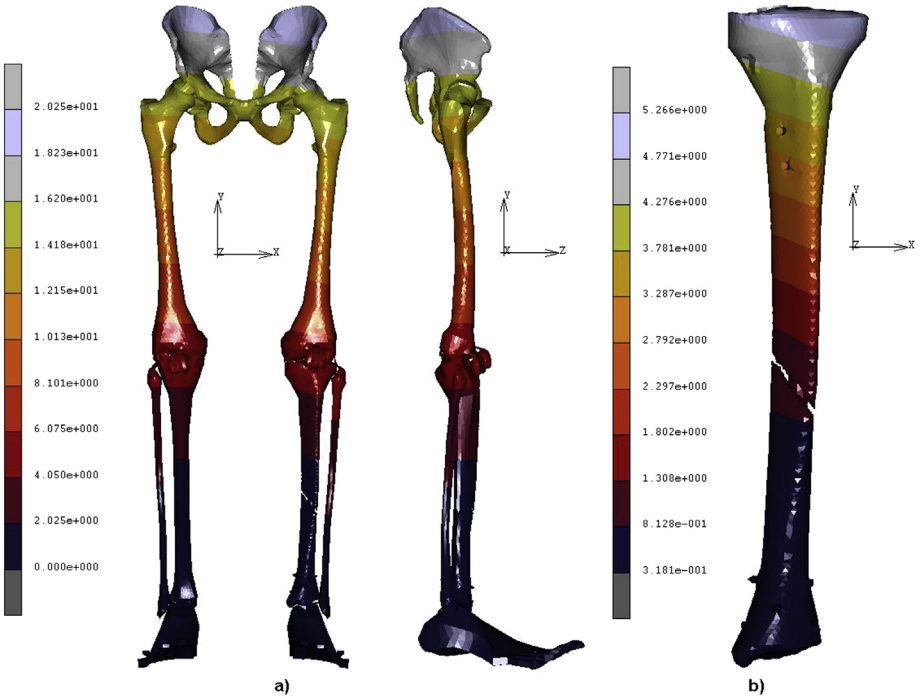

Fig. 5 – Contour maps of Displacements localized on: a) the complete model b) the fractured tibia.

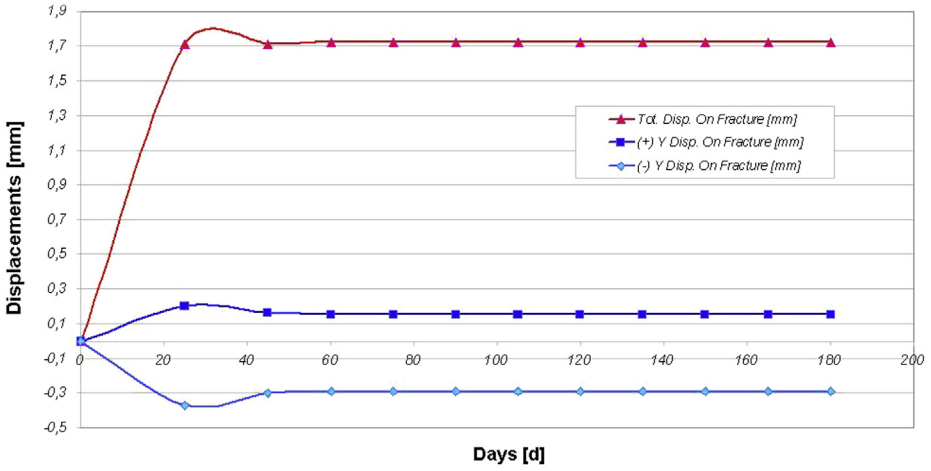

Fig. 6 – Curves of total displacements and displacements along the Y axes Vs Days (or equivalent percentage of the elastic modules) for the fractures.

show a large amount of shear compared to compression. In fact, it is well-known that the mechanical conditions during the early phase of bone healing modify the course of healing and the quality and quantity of callus formation.[46,47] Moreover, the differences observed in shear interfragmentary strains may also delay the fracture healing process.[48] This is especially relevant in distal and mid-diaphyseal fractures stabilized by an unreamed intramedullary nail, where differences up to 50% were found. An intact fibula enhances mechanical stability and prevents sliding of the fracture components when the interlocking screws are removed. The prevalence of compressive strains at the postero-medial cortex and the relative tension of the antero-lateral cortices suggested a combined loading consisting of axial compression superimposed onto bending in the mid–sagittal plane. In vitro gauge measurements of intact tibiae under simplified loading showed strain magnitudes ageing between 125 and 220 mΣ, while in the present research was obtained an equivalent elastic strain on the tibia ageing from 154 to 222 [mΣ], and a value of 63 [mΣ] localised on the fracture site, for the healed tibia. From the computational analysis of the healthy tibia, compressive strains in the postero-medial side of the tibia indicated a combined axial compression and bending mode onto the mid–sagittal plane.[49] Similarly, Goodwin and Sharkey,[50] performed a gait simulation and measured peak strains on the surface of the distal third of the tibial diaphysis of 431 to 310 mΣ, in compression, and from 719 to 469 mΣ in tension. The most important differences are observed in shear interfragmentary strains for fractures stabilized by an unreamed nail. The equivalent elastic strain on the nail body has a peak in the case of the fractured tibia 67 [mΣ], and then follows an increasing trend from 50 to 52 [mΣ]. The equivalent elastic strain registered on the superior and inferior screws follow increasing courses respectively ageing from 11 to 26 [mΣ], for the superior screws, and from 8 to 25 [mΣ] for the inferior ones.

5. Conclusions

The extended usage of unreamed tibial nailing resulted in reports of an increased rate of complications, especially for the distal portion of the tibia. Intramedullary nailing of a tibial

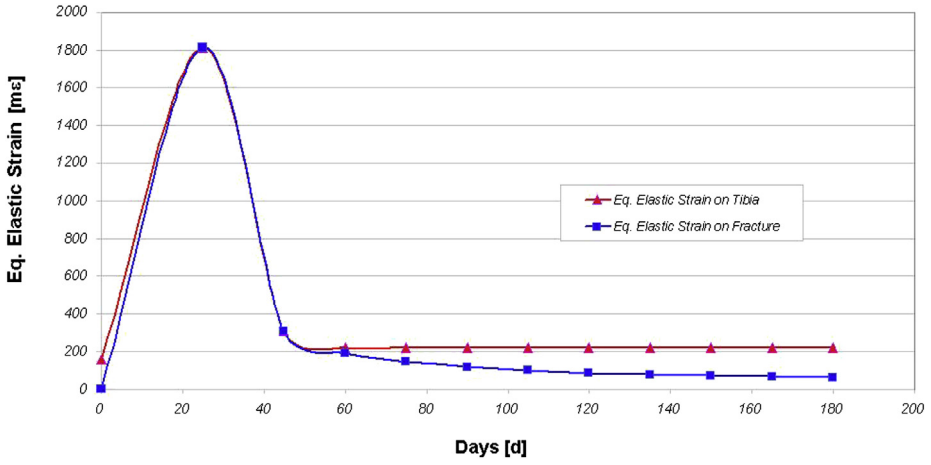

Fig. 7 – Curves of Eq. Elastic Strain Vs Days (or equivalent percentage of the elastic modulus) for the fractured Tibia and Fracture.

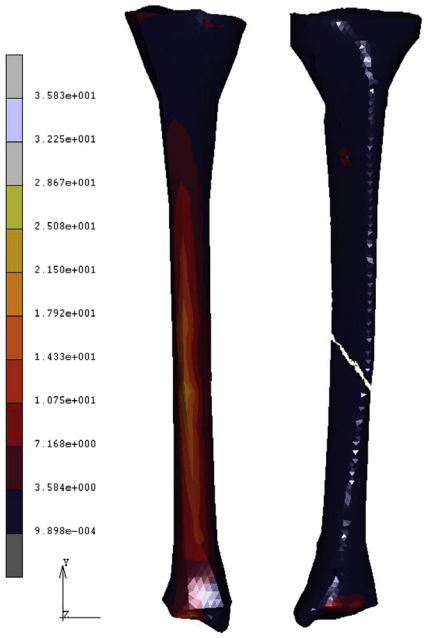

Fig. 8 – Comparison between the healthy tibia and the fractured one, in terms of eq. V. Mises Stress.

fracture at any level has been associated with complications such as an increased risk of compartment syndrome, nail breakage and most commonly, chronic knee pain, which often persists beyond removal of the nail. The goal of this work was to gain a thorough understanding of the load-sharing mechanism between unreamed Expert Tibial (DePuy Synthes®) Nail and bones in a fractured tibia. The obtained results reveal that after a brief period of re-calcification, estimated in 30–40 the mechanical behaviour of the implanted tibia is almost the same of the healed one, in terms of eq. V. Mises Stress, displacements, and strains. The problem could be investigated further by taking into account, from a chemical and biological point of view, the robustness and the durability of the new bony structure just created around the fracture site. Other interesting consequences were investigated by taking into account how the stress and strain shielding can influence the integrity and resistance of bones. Although the numerical approach does not fully simulate physiological loading and only roughly imitates the effect of ligaments, fasciae, compartments and other soft tissue structures, it seemed to offer a good approximation. Knowledge on the behaviour of implants under physiological conditions is essential to understand their performance in vivo. Pre-clinical testing of osteosynthetic devices should include beside strength testing and stiffness evaluation an analysis of the load-sharing mechanisms under physiological-like loading conditions. Nailing a fractured tibia results for all defect locations in a considerable unloading of the bone during normal gait. By this, the bone structure even if is distant from the fracture site is subjected to a modified mechanical loading compared with the intact situation. In patients with osteoporosis or otherwise reduced bone stock, this mechanical unloading might lead to a further pronounced effect of bone resorption. The large interfragmentary strain observed for the distal defect locations provide a biomechanical explanation for the large failure rate seen in unreamed nailing of distal shaft fractures, especially in those cases without appropriate bony support. The evolution of treatment options for these fractures has been closely linked to developments in implant technology and surgical technique.

Conflicts of interest

The author has none to declare.

REFERENCES

1. Horne G, Iceton J, Twist J, et al. Disability following fractures of the tibial shaft. *Orthopedics*. 1990;13:423–426.
2. Hooper GJ, Keddell RG, Penny ID. Conservative management or closed nailing for tibial shaft fractures. A randomised prospective trial. *J Bone Joint Surg Br*. 1991;73:83–85.
3. Haas N, Schutz M, Sudkamp N, Hoffmann R. The new unreamed AO nails for the tibia and the femur. *Acta Orthop Belg*. 1995;61:204–206.
4. Claes L, Wilke HJ, Augat P, Rubenacker S, Margevicius KJ. Effect of dynamization on gap healing of diaphyseal fractures under external fixation. *Clin Biomech*. 1995;10:227–234.
5. Burger EH, Veldhuijzen JP. Influence of mechanical factors on bone formations, resorption and growth in vitro. In: Hall BK, ed. *Bone*. Boca Raton, FL: CRC Press; 1993:37–56.
6. Goodship AE, Kenwright J. The influence of induced micro-movement upon the healing of experimental tibial fractures. *J Bone Joint Surg Br*. 1985;67-B:650–655.
7. Kenwright J, Richardson JB, Cunningham JL, et al. Axial movement and tibial fractures. A controlled randomized trial of treatment. *J Bone Joint Surg Br*. 1991;73-B:654–659.
8. Mueller CA, Eingartner C, Schreitmueller E, et al. Primary stability of various forms of osteosynthesis in the treatment of fractures of the proximal tibia. *J Bone Joint Surg Br*. 2005;87:426–432.
9. Markmiller M, Tjarksen M, Mayr E, et al. The unreamed tibia nail. Multicenter study of the ao/asif. Osteosynthes fragen/association for the study of internal fixation. *Langenbecks Arch Surg*. 2000;385:276–283.
10. Schemitsch E, Kowalski M, Swiontkowski M, et al. Cortical bone blood flow in reamed and unreamed locked intra medullary nailing: a fractured tibia model in sheep. *J Orthop Trauma*. 1994;8:373–382.
11. Klein M, Rahn B, Frigg R, et al. Reaming versus nonreaming in medullary nailing: interference with cortical circulation of the canine tibia. *Arch Orthop Trauma Surg*. 1990;109:314–316.
12. Boenisch UW, De Boer PG, Journeaux SF. Unreamed intra medullary tibial nailing-fatigue of locking bolts. *Injury*. 1996;27:265–270.
13. Court-Brown CM, Will E, Christie J, et al. Reamed or unreamed nailing for closed tibial fractures. A prospective study in t scherne c1 fractures. *J Bone Joint Surg Br*. 1996;78-B:580–583.
14. Turner CH, Anne V, Pidaparti RMV. A uniform strain criterion for trabecular bone adaptation: do continuum-level strain gradients drive adaptation? *J Biomechanics*. 1997;30:555–563.
15. Lewis G, Holland D. Geometrical properties and torsional fatigue life of a tibial interlocking intramedullary nail segment. *J Orthop Trauma*. 1998;12:8–15.
16. Schandelmaier P, Krettek C, Tscherne H. Biomechanical study of nine different tibia locking nails. *J Orthop Trauma*. 1996;10:37–44.
17. Thomas KA, Bearden CM, Gallagher DJ, Hinton MA, Harris MB. Biomechanical analysis of nonreamed tibial intra-medullary

nailing after simulated transverse fracture and fibulectomy. *Orthopedics*. 1997;20:51–57.
18. Hutson JJ, Zych GA, Cole JD, et al. Mechanical failures of intramedullary tibial nails applied without reaming. *Clin Orthop*. 1995;315:129–137.
19. Blachut PA, O'Brien PJ, Meek RN, Broekhuyse HM. Interlocking intramedullary nailing with and without reaming for the treatment of closed fractures of the tibial shaft. A prospective, randomized study. *J Bone Joint Surg Am*. 1997;79-A:640–646.
20. Freedman EL, Johnson EE. Radiographic analysis of tibial fracture malalignment following intra-medullary nailing. *Clin Orthop*. 1995;315:25–33.
21. Vrahas M, Fu F, Veenis B. Intraarticular contact stresses with simulated ankle malunions. *J Orthop Trauma*. 1994;8:159–166.
22. Raunest J, Kynast W, Lesch V, et al. Geometric properties of the fractured tibia stabilized by unreamed interlocking nail: development of a three-dimensional finite element model. *Comp Biomed Res*. 1996;29:259–270.
23. Duda GN, Heller M, Albinger J, Schulz O, Schneider E, Claes L. Influence of muscle forces on femoral strain distribution. *J Biomechanics*. 1998c;31:841–846.
24. Schmidt AH, Finkemeier CG, Tornetta P. Treatment of closed tibial fractures. *J Bone Joint Surg*. 2003;85A:351–368.
25. Kumar A, Charlebois SJ, Cain EL, et al. Effect of fibular plate fixation on rotational stability of simulated distal tibial fractures treated with intra-medullary nailing. *J Bone Joint Surg*. 2003;85A:604–608.
26. Lambert KL. The weigh-bearing function of the fibula. *J Bone Joint Surg*. 1971;53A:507–513.
27. Sonoda N, Chosa E, Totoribe K, et al. Biomechanical analysis for stress fractures of the anterior middle third of the tibia in athletes: nonlinear analysis using a three dimensional finite element method. *J Orthop Sci*. 2003;8:505–513.
28. Goldhahn S, Bigler R, Moser R, Matter P. Therapie und Komplikations management bei Tibia-Schaftfrakturen in der Schweiz. *Hrz Unfallchirug*. 1999;275:449–450.
29. Lang GJ, Cohen BE, Bosse MJ, Kellam JF. Proximal third tibial shaft fractures. Should they be nailed? *Clin Orthop*. 1995;315:64–74.
30. Henley MB, Chapman JR, Agel J, Harvey EJ, Whorton AM, Swiontkowski MF. Treatment of type II, IIIA, and IIIB open fractures of the tibial shaft: a prospective comparison of unreamed interlocking intra-medullary nails and half-pin external fixators. *J Orthop Trauma*. 1998;12:1–7.
31. Hayes WC, Swenson LW, Schurman DJ. Axisymmetric finite element analysis of the lateral tibial plateau. *J Biomechanics*. 1978;11:21–33.
32. Filardi V. Stress schielding in the bony chain of leg in presence of varus or valgus knee. *J. Orthop*. 2014.
33. Filardi V. FE analysis of stress and displacements occurring in the bony chain of leg. *J. Orthop*. 2014:157–165.
34. Krettek C, Schandelmaier P, Rudolf J, Tschetrne H. Current status of surgical technique for unreamed nailing of tibial shaft fractures with the UTN (unreamed tibia nail). *Unfallchirurg*. 1994;97:575–599.
35. Hahn D, Bradbury N, Hartley R, Radford PJ. Intramedullary nail breakage in distal fractures of the tibia. *Injury*. 1996;27:323–327.
36. Nork SE, Schwartz AK, Agel J, et al. Intramedullary nailing of distal metaphyseal tibial fractures. *J Bone Joint Surg Am*. 2005;87-A:1213–1221.
37. Robinson CM, McLauchlan GJ, McLean IP, Court-Brown CM. Distal metaphyseal fractures of the tibia with minimal involvement of the ankle. *J Bone Joint Surg Br*. 1995;77-B:781–787.
38. Duda GN, Mandruzzato F, Heller M, et al. Mechanical boundary conditions of fracture healing: borderline indications in the treatment of unreamed tibial nailing. *J Biomech*. 2001;34:639–650.
39. Rohlmann A, Mossner U, Bergmann G, Kolbel R. Finite element-analysis and experimental investigation of stresses in a femur. *J Biomed Eng*. 1982;4:241–246.
40. Rybicki EF, Simonen FA, Weis EB. On the mathematical analysis of stress in the human femur. *J Biomechanics*. 1972;5:203–215.
41. Gomez-Benito MJ, Fornells P, Garcia-Aznar JM, et al. Computational comparison of reamed versus unreamed intramedullary tibial nails. *J Orthop Res*. 2007;25:191–200.
42. Gardner TN, Evans M, Hardy J, Kenwright J. Dynamic interfragmentary motion in fractures during routine patient activity. *Clin Orthop*. 1997;336:216–225.
43. Hopf T, Harnroongroi T. Biomechanical studies of the role of the interfragmentary traction screw in plate osteosynthesis exemplified by a short oblique tibial shaft fracture. *Aktuelle Traumatol*. 1986;16:60–66.
44. Yamagishi M, Yoshimura Y. The biomechanics of fracture healing. *J Bone Joint Surg Am*. 1955;37-A:1035–1068.
45. Gardner TN, Evans M, Kenwright J. The influence of external fixators on fracture motion during simulated walking. *Med Eng Phys*. 1996;18:305–313.
46. Djahangiri A, Garofalo R, Chevalley F, et al. Closed and open grade I and II tibial shaft fractures treated by reamed intramedullary nailing. *Med Princ Pract*. 2006;15:293–298.
47. Egol K, Wolinsky P, Koval KJ. Open reduction and internal fixation of tibial pilon fractures. *Foot Ankle Clin*. 2000;5:873–885.
48. Egol KA, Weisz R, Hiebert R, et al. Does fibular plating improve alignment after intramedullary nailing of distal metaphyseal tibia fractures? *J Orthop Trauma*. 2006;20:94–103.
49. Bourne RB. Pylon fractures of the distal tibia. *Clin Orthop Relat Res*. 1989;240:42–46.
50. Goodwin KJ, Sharkey NA. Material properties of interstitial lamellae reflect local strain environments. *J Orthop Res*. 2002;20:600–606.